Bioorganic & Medicinal Chemistry 20 (2012) 4954–4961

Contents lists available at SciVerse ScienceDirect

Bioorganic & Medicinal Chemistry

journal homepage: www.elsevier.com/locate/bmc

Design and synthesis of marine fungal phthalide derivatives as PPAR-γ agonists

Bin Xiao [a], Jun Yin [b], Minhi Park [a], Juan Liu [c], Jian Lin Li [a], Eun La Kim [a], Jongki Hong [d], Hae Young Chung [a], Jee H. Jung [a,*]

[a] College of Pharmacy, Pusan National University, Busan 609-735, Republic of Korea
[b] College of Traditional Chinese Materia Medica, Shenyang Pharmaceutical University, Shenyang 110016, China
[c] South China Sea Institute of Oceanology, Chinese Academy of Sciences, Guangzhou 510301, China
[d] College of Pharmacy, Kyung Hee University, Seoul 130-701, Republic of Korea

ARTICLE INFO

Article history:
Received 31 May 2012
Revised 21 June 2012
Accepted 21 June 2012
Available online 29 June 2012

Keywords:
PPAR-γ
Phthalide
Marine fungus
Binding assay
Luciferase assay

ABSTRACT

On the basis of a marine fungal phthalide (paecilocin A) skeleton, we synthesized 20 analogs and evaluated them for peroxisome proliferator-activated receptor gamma (PPAR-γ) binding and activation. Among these analogs, **6** and **7** had significant PPAR-γ binding activity, and **7** showed further PPAR-γ activation in rat liver Ac2F cells. In docking simulation, **7** formed H bonds with key amino acid residues of the PPAR-γ binding domain, and the overall positioning was similar to rosiglitazone. This new phthalide derivative is considered an interesting new molecular class of PPAR-γ ligands.

1. Introduction

Peroxisome proliferator-activated receptors (PPARs) are members of the nuclear receptor superfamily of ligand-activated transcription factors and include three isoforms: α, β/δ, and γ.[1–4] PPAR-γ is the most abundant isoform in adipose tissue, macrophages, monocytes, intestinal cells, skeletal muscle, and endothelium, and plays an important role in the regulation of insulin sensitivity, lipid metabolism, adipogenesis, and glucose homeostasis.[5] Thiazolidinediones (TZDs) such as rosiglitazone, pioglitazone, and ciglitazone are high-affinity ligands and full agonists of PPAR-γ that are used in the treatment of type 2 diabetes mellitus.[6–8] Because if the adverse effects asociated with PPAR-γ ligands, such as weight gain, edema, and fluid retention, discovery of new PPAR-γ ligands that do not have adverse effects is essential in the development of new therapeutics for insulin resistance and type 2 diabetes mellitus.[9]

A ternary complex structure (2PRG) composed of the PPAR-γ ligand-binding domain (LBD), rosiglitazone, and human steroid receptor co-activating factor-1 (SRC-1) was described in 1998.[10] The PPAR-γ LBD contains a large binding pocket that allows diverse types of ligands to enter and search for their proper laying conformations for ligand–receptor complexes. In addition to TZDs and L-tyrosine analogs, natural fatty acids such as docosahexaenoic acid (DHA), eicosapentaenoic acid (EPA), and cyclopentenone prostaglandin (15d-PGJ_2), are also reported to be PPAR-γ agonists with relatively low affinities.[11] PPAR-γ agonists consist of a hydrophilic head group tethered to an aromatic center linked to a hydrophobic tail. The hydrophilic head group typically has hydroxyl, carbonyl, or carboxyl oxygen atoms (e.g., carboxylic acid and 2, 4-thiazolidinedione), which form H bonds with the key amino acid residues (Tyr473, His449, His323, and Ser289) of the PPAR-γ LBD. These H bonds stabilize PPAR-γ in the proper conformation, which is crucial for successful co-activator recruitment.[12,13] The aromatic center forms a variety of Van der Waals interactions with various hydrophobic residues in the LBD, and the hydrophobic tail tolerates a more diverse set of substituents that are free to interact with the fairly large hydrophobic pocket as well as water molecules in it.[14] These are graphically illustrated in Figure 1 as a key pharmacophore concept in terms of rosiglitazone, a potent and selective PPAR-γ agonist.

In the course of our search for bioactive marine natural products, new phthalide derivatives paecilocins A–C (Fig. 2A) were isolated from the jellyfish-derived fungus *Paecilomyces variotii*.[15] In a subsequent screening for PPAR-γ competitive binding activity, paecilocin A showed activity comparable to that shown by rosiglitazone (Fig. 2B). Other similar structures 3-butyl-1(3*H*)-isobenzofuranone, 3-butylidenephthalide, and senkyunolide B are covered in a patent as effective agents for the prevention or treatment of

* Corresponding author. Tel.: +82 51 5102803; fax: +82 51 5136754.
E-mail address: jhjung@pusan.ac.kr (J.H. Jung).

0968-0896/$ - see front matter © 2012 Elsevier Ltd. All rights reserved.
http://dx.doi.org/10.1016/j.bmc.2012.06.039

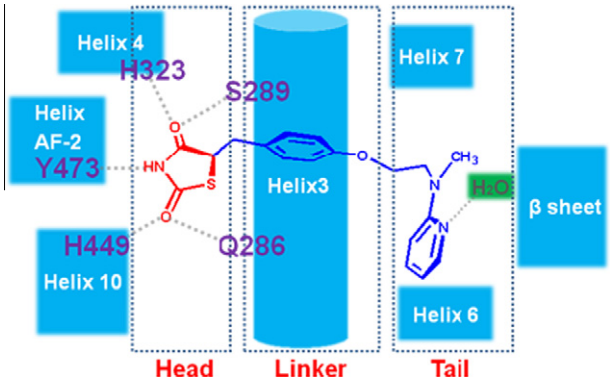

Figure 1. Graphical illustration of the key pharmacophore concept of rosiglitazone. The rosiglitazone skeleton is divided into the head, linker, and tail by dashed line boxes. Key helices and sheets (light blue), amino acid residues (purple), hydrogen bonds (gray dashed line), and water molecule (in green) of PPAR-γ LBD are shown.

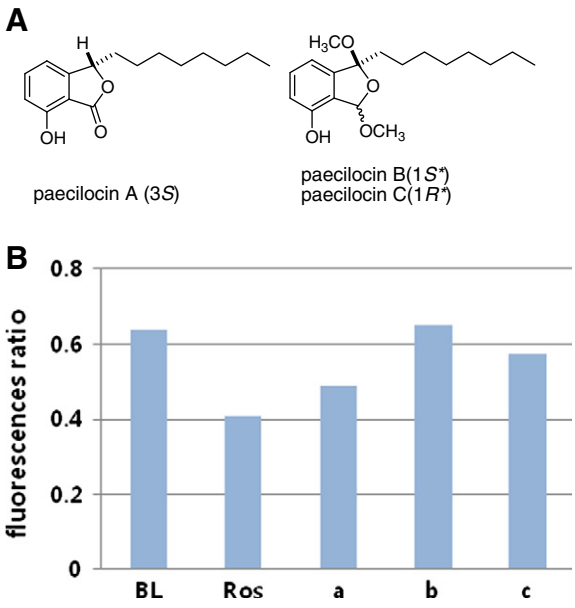

Figure 2. Chemical structures (A) and PPAR-γ binding activity (B) of fungal phthalides. Activity was measured using LanthaScreen TM TR-FRET PPAR-γ competitive binding assay. BL (blank control, without PPAR-γ LBD), Ros (rosiglitazone). Rosiglitazone and phthalide analogs **a**–**c** (paecilocins A–C, respectively) were assayed at 100 μM. The fluorescence ratio at 520/495 nm is shown.

diabetes mellitus and the mechanism of action was speculated to be PPAR-γ activation.[16] Motivated by these preliminary findings, we synthesized paecilocin A racemate and its analogs to characterize a new PPAR-γ agonistic skeleton.

2. Results and discussion

2.1. Chemistry

Paecilocin A can be synthesized in at least 5 steps by applying a reported scheme.[17] For a preliminary study, a racemic mixture of paecilocin A as well as a series of derivatives were synthesized according to a reported single-step scheme.[18] Considering the pharmacophore analyses of rosiglitazone, the carbonyls or hydroxyls and the hydrophobic alkyl chain were retained on the head group and as a tail group, respectively.

Commercially available 3-hydroxy phthalic anhydride (**1**) was treated with the nucleophilic Grignard reagent octylmagnesium bromide to generate a mixture of differently alkylated products **2**–**7** (Scheme 1). Monoalkyl derivatives (**2** and **3**) were obtained as the major products. Simultaneous alkylation did not occur on both carbonyls. However, 2 alkyl chains easily attached to a single carbonyl carbon (**4** and **5**). Continuous treatment with HCl produced dehydroxy derivatives **6** and **7** (paecilocin A racemate). Compound **3** was treated with benzyl chloride to yield hydroxy-substituted analogs. In addition, a mixture of benzyl derivatives (**9** and **10**) was obtained. Further treatment of **10** with MeI generated derivative **11**, with the free hydroxyl group blocked as a methoxyl group. Compound **8** was produced from **7** by using the same procedure. Compounds **13** and **14**, without hydroxyls in the benzene ring, were obtained in a mixture by the reaction of commercially available phthalic anhydride (**12**) with octylmagnesium bromide. In this case, the dialkyl derivative (**14**) was obtained as a major product and the monoalkyl derivative (**13**) was obtained as a minor component (Scheme 2).

In the presence of H_2O and heat, commercially available phthalic anhydrides (**1** and **16**) were hydrolyzed to *ortho*-phthalic acids (Scheme 2).[19] To retain the free carboxyl on the benzene ring as a ligand head, the *ortho*-phthalic acids were treated with 1-bromooctane, and the octyl phthalates **15** and **17** were produced (Scheme 2). The etherification selectively proceeded on the *meta*-carboxyl group, possibly due to the intra-molecular H bond formation between the phenolic hydroxyl or nitro group with the *ortho*-carboxyl group. Treatment of **1** with 1-bromooctane yielded phthalic anhydride 3-octyl ether. Subsequent treatment with MeOH and heat yielded a mixture of methyl esters (**18** and **19**) in similar yields. Compound **20** was produced by treating **1** with decanoyl chloride to yield a TZD-mimic pharmacophore with dione as a head and a long acyl chain as the hydrophobic tail (Scheme 2).

2.2. PPAR-γ binding activity

All synthesized compounds were compared with rosiglitazone for their binding affinity to the PPAR-γ LBD (Fig. 3). Compounds **6** and **7** showed significant binding, comparable to that shown by rosiglitazone. Of the three different phthalic anhydride heads (**1**, **12**, and **16**), only **1** showed activity while **12** and **16** showed no notable activity. This suggested the importance of the hydroxyl group on the benzene ring. When the hydroxyl group was blocked by benzyl or methyl groups (**8**, **9**, **10**, and **11**), the binding ability diminished. Additionally, the substitution of a bulky group at the stereo-center (**2**–**5** and **9, 10**, and **11**) was detrimental to the activity, indicating that introduction of a third arm on the benzene ring did not enhance activity.[6–8]

Among the open phthalate analogs (**15**, **17**, **18**, and **19**), compounds **15** and **17** exhibited better activity, indicating that the free carboxyl moiety and additional H bond donor or acceptor (such as the hydroxyl or nitro group on the head) were valuable for binding the PPAR-γ LBD. The imitation structure (**20**) of classic pharmacophore of TZDs did not show activity enhancement compared to the simple phthalic anhydride (**1**). The preliminary SAR of each phthalide derivative is summarized in Figure 4.

Interestingly, compared to rosiglitazone, the synthetic racemate (**7**) displayed better binding activity than natural paecilocin A (Figs. 2B and 3). This suggests that the enantiomer (*R*-isomer, **7**-***R***) of paecilocin A (*S*-isomer, **7**-***S***) might be a better ligand for PPAR-γ. Therefore, enantiomeric structures of paecilocin A (**7**-***R*** and **7**-***S***) as well as **6** and rosiglitazone were evaluated for receptor binding by docking simulation to collect supplementary data.

2.3. Molecular docking study

PPAR-γ has been a challenging target for molecular modeling for several reasons. First, the binding site is large, and the ligand

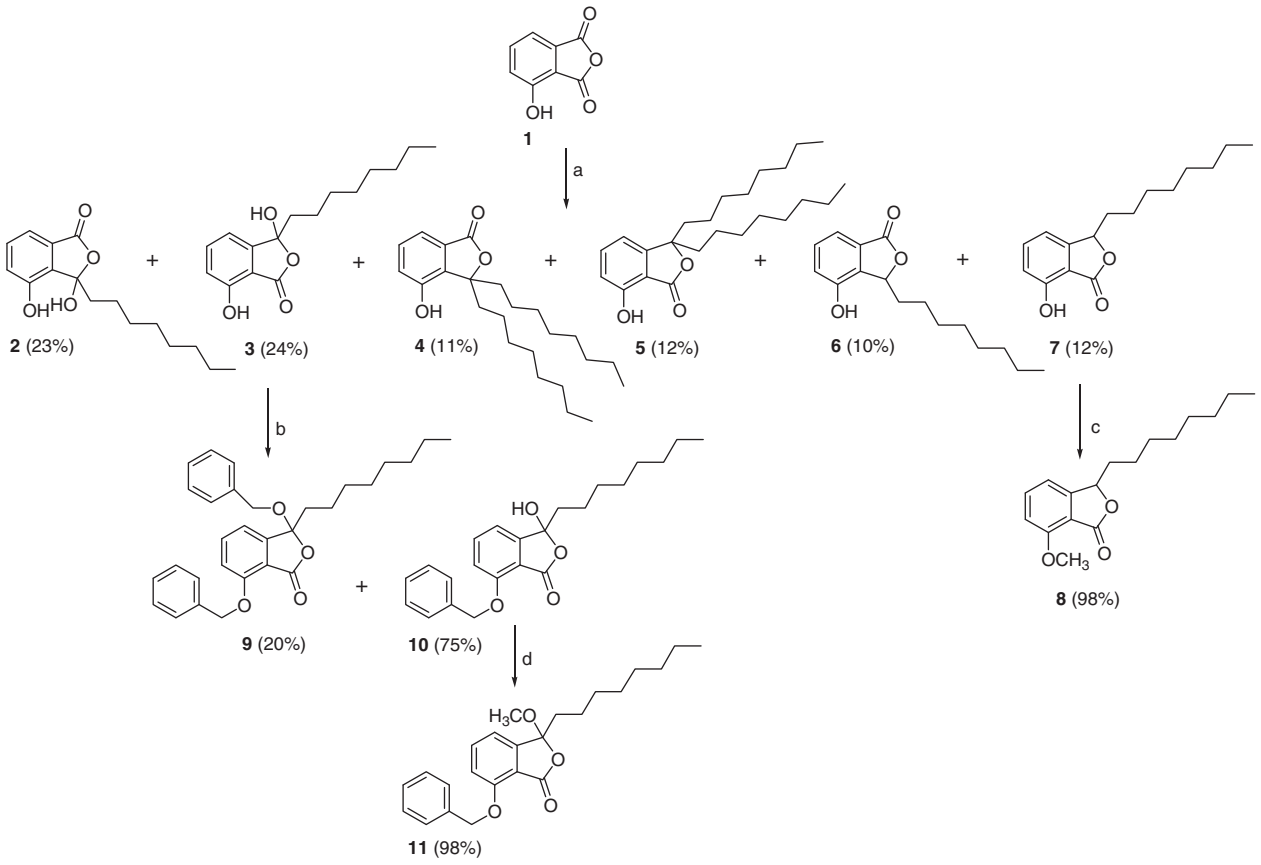

Scheme 1. Reagents and conditions: (a) $Me(CH_2)_7MgBr$, THF, −20 °C, stir, 2 h; 1 M HCl, stir, 0.5 h; (b) benzyl chloride, K_2CO_3, NaI, DMF, stir, rt, 4 h; (c) MeI, Ag_2O, stir, 12 h; (d) MeI, Ag_2O, stir, 12 h.

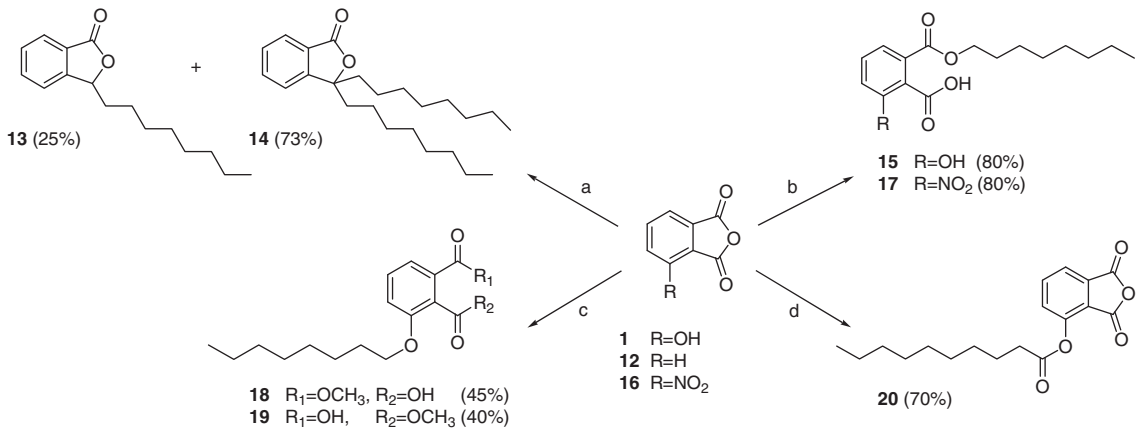

Scheme 2. Reagents and conditions: (a) $Me(CH_2)_7MgBr$, THF, −20 °C, stir, 2 h; 1 M HCl, stir, 0.5 h; (b) aq. CH_3CN $Me(CH_2)_7Br$, Ag_2O, aq. CH_3CN 80 °C, stir, 12 h; (c) $Me(CH_2)_7Br$, Ag_2O, 80 °C, stir, 12 h; Methanol, 35 °C 0.3 h; (d) decanoyl chloride, stir, 0–15 °C, 4 h.

tail is always located in a big hydrophobic pocket that does not interact with amino acid residues to contribute to its biological activity. Next, the binding is considered flexible and in particular, the side chains move significantly upon ligand binding. Finally, the binding site is highly lipophilic, which presents a challenge for structure-based approaches.[10,14,20,21]

On the basis of these characteristics and the large amount of available experimental data, we were able to apply more sophisticated docking workflow. The crystal structure of the 2PRG complex was re-docked for validation. Because a low root mean square deviation (RMSD) value does not necessarily correspond to a docking pose that renders the most crucial ligand–protein interactions, we did not rely only on the RMSD value for validating the docking workflow. Instead, we used PyMol v1.5 for analysis and investigation of the ligand–protein interactions of the docking poses.[22]

The crystal form of 2PRG contains 2 molecules in the asymmetric unit, denoted A and B. Only chain A was proposed to represent a realistic model for the activated PPAR-γ protein.[20] For chain B, most re-docking modes lacked the key interactions with His449 and Glu286. However, re-docking with chain A allowed most crucial ligand–protein interactions to occur. Therefore, chain A was selected for the PPAR-γ agonist docking workflow. Re-docking of rosiglitazone was performed with different water molecules in the hydrophobic binding pocket, and H_2O308, H_2O339, H_2O444,

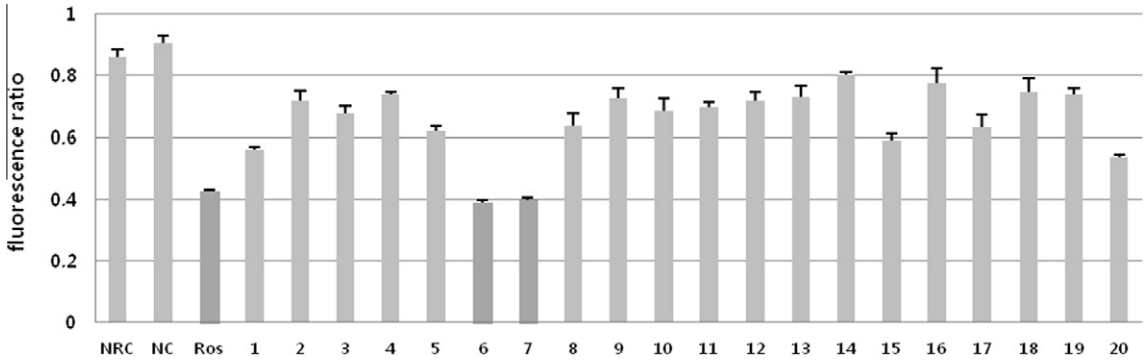

Figure 3. Measurement of the in vitro PPAR-γ binding activity of phthalide analogs by using the LanthaScreen™ TR-FRET PPAR-γ competitive binding assay. NRC (no receptor control, without PPAR-γ LBD), NC (negative control, with solvent DMSO), Ros (rosiglitazone). Rosiglitazone and phthalide analogs were assayed at 50 μM. The fluorescence ratio at 520/495 nm is shown as the mean + s.d. (n = 3).

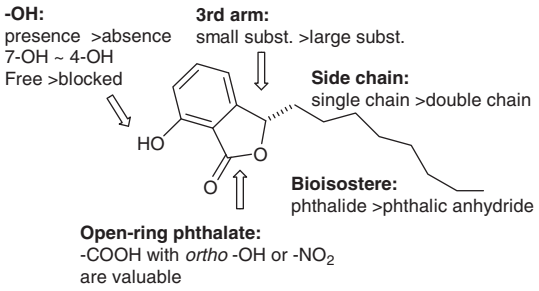

Figure 4. Structure–activity relationship of phthalide derivatives.

and H_2O467 were finally selected. This generated top-ranked and reproducible binding modes that are close to those in the 2PRG crystal.

The enantiomer **7-*R*** ranked over **7-*S*** (paecilocin A) and was likely to form H bonds with Tyr473, His449, His343, Ser289, and Glu286 in the PPAR-γ LBD. This is highly similar to the H bonding network of rosiglitazone in 2PRG. The enantiomer **7-*S*** lacked interaction with His449. However, their affinities were not significantly different (-7.0 kcal/mol for **7-*S*** and -6.9 kcal/mol for 7-***R***), but were higher than **6** (-6.4 kcal/mol) (Fig. 5). Not only binding affinity but also other factors such as H bonding with key amino acid residues would be important for activation of PPAR-γ. More H bonds would be helpful to 'lock' PPAR-γ protein in an active conformation which is preferable for the co-activator recruitment and further activation. Compound **7-*S*** lack two H bonds compared to **7-*R***, especially the H bond between hydroxyl oxygen and His449 on the helix 10, which is crucial for the lock of this helix as well as the whole protein. The enantiomer **6-*R*** ranked over **6-*S*** and formed H bonds with Tyr473, His343, and Ser289 of the PPAR-γ LBD. Simulation data revealed that **7-*R*** and **7-*S*** bind PPAR-γ more preferentially than **6**, and **7–*R*** was a better ligand than **7-*S***. The enantiomer **7-*R*** is considered to be anchored by the H bonding network in the Y-shaped binding pocket of PPAR-γ and stabilizes the protein like a mouse trap, which is the preferable conformation for co-activator binding. The asymmetric carbon atom acts like a switch, and the *R* configuration could force the lipophilic alkyl chain to fill the hydrophobic portions of the pocket in a preferable pose as well as stabilize the head group in a direction to furnish the bonding network.[23] Because the correlation of experimental affinity data and scoring functions is controversial, the best docking modes for the PPAR-γ ligands were selected by taking the docking scores as well as the results of the visual investigation into account.[24–26] Compounds **6** and **7** were subsequently evaluated for PPAR-γ activation in Ac2F cells.

2.4. PPAR-γ activation

Compounds **6** and **7** were evaluated using luciferase transactivation assays in rat liver Ac2F cells transiently transfected with pcDNA3/pFlag-PPAR-γ1 and PPRE. In contrast to the binding assay results (Fig. 3), **6** and **7** were less active than rosiglitazone. However, compound **7** had activity that increased in a concentration-dependent manner (Fig. 6).

The intra-molecular H bond of compound **7** might modulate lipophilicity and lead to cell permeability differences between **6** and **7** in Ac2F cells. Moreover, competitive binding and activation of PPAR-γ might involve different mechanisms. Under competitive binding conditions, **6** and **7** could similarly displace the fluorescent pan PPAR-γ agonist from the PPAR-γ LBD. In the transactivation assay, however, the changed conformation of the PPAR-γ protein by different ligands (**6** and **7**) should be different, and this could lead to different degrees of co-activator recruitment. Other factors might be also involved in bioavailability modulation of these molecules in vivo. Therefore, further optimization and in vivo evaluation of these molecules would provide valuable data.

3. Conclusion

In this study, a series of fungal phthalide-based analogs were prepared and evaluated for PPAR-γ binding and activation. Compound **7** showed significant PPAR-γ binding and moderate PPAR-γ activation in rat liver Ac2F cells. Compound **7** formed H bonds with key amino acid residues of the PPAR-γ LBD, and its overall positioning in the binding pocket was similar to that of rosiglitazone. The slightly higher binding activity of the synthetic racemate (**7**) over the natural molecule (paecilocin A, **7-*S***) was verified by molecular docking experiments and the **7-*R*** isomer was considered a more favorable ligand. These new phthalide derivatives are considered an interesting new molecular class of PPAR-γ ligands, and the asymmetric synthesis of pure enantiomers and further biological evaluation would provide valuable information.

4. Experimental section

4.1. Chemistry

The ^1H and ^{13}C NMR spectra were recorded on Varian Unity 400 MHz NMR spectrometer. The chemical shifts are reported with reference to the respective residual solvent or deuterated solvent

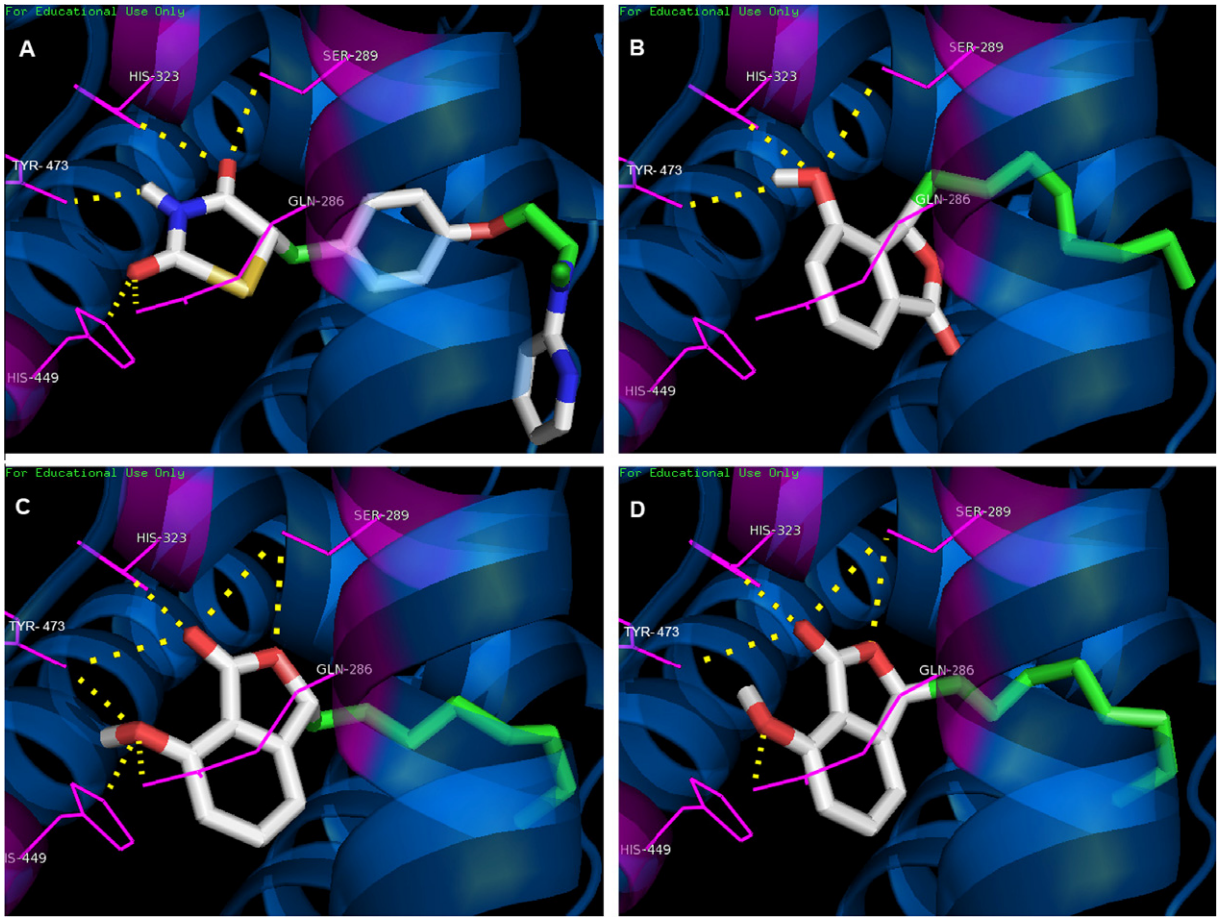

Figure 5. The 3D putative binding modes of rosiglitazone, **6**-***R***, and **7**-***R*/*S*** with PPAR-γ LBD. (A) Rosiglitazone interacts with key amino acid residues (Tyr473, His449, His343, Ser289, and Glu286) in the PPAR-γ binding pocket (−8.2 kcal/mol); (B) binding mode of **6**-***R*** (−6.4 kcal/mol); (C) binding mode of **7**-***R*** (−6.9 kcal/mol); (D) binding mode of **7**-***S*** (−7.0 kcal/mol).

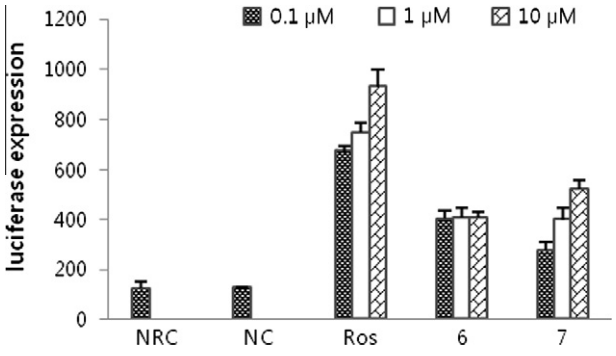

Figure 6. In vitro PPAR-γ activation by **6** and **7** in rat liver Ac2F cells. Cells were transiently transfected with pcDNA or PPRE with pFlag-PPAR-γ1. NRC (no receptor control, without transfection of plasmid), NC (negative control, transfected with plasmid with PPRE and pcDNA), Ros (rosiglitazone). Rosiglitazone was used as positive control to monitor the activation of the luciferase reporter. Luciferase expression (RLU/well) is shown as the mean + s.d. ($n = 5$). RLU; relative light unit.

peaks (δ_H 3.30 and δ_C 49.0 for CD_3OD, δ_H 7.24 and δ_C 76.8 for $CDCl_3$). The FAB MS data was obtained on a JEOL JMS SX-102A spectrometer. HPLC was performed on a YMC ODS-H80 column (250 × 10 mm, 4 μm, 80 Å) and a C18-5E Shodex packed column (250 × 10 mm, 5 μm, 100 Å) by using a Shodex RI-71 detector. All chemical reagents were purchased from Sigma-Aldrich and used as received.

4.2. General procedure for the synthesis of phthalide derivatives

4.2.1. Preparation of 2–7

To a solution of 3-hydroxyphthalic anhydride (**1**) in THF at −20 °C, octylmagnesium bromide (2.5 equiv) in THF was added, and the mixture was stirred for 15 min and warmed to room temperature for another 2 h. The reaction was quenched with 1 M HCl and concentrated in vacuo. The residue was diluted with EtOAc and successively washed with H_2O and brine. The organic layer was dried with $MgSO_4$ and evaporated to obtain a crude product, which was purified by RP HPLC eluting with 80% aqueous MeOH to give **2**–**7**. Compound **2** (23%): White powder; ^{1}H NMR (CD_3OD, 400 MHz): δ 0.83 (t, J = 7.2 Hz, 3H), 1.18–1.26 (m, 12H), 2.32 (brs, 2H), 7.05 (d, J = 8.4 Hz, 1H), 7.27 (d, J = 7.2 Hz, 1H), 7.36 (t, J = 7.6 Hz, 1H); ^{13}C NMR (CD_3OD, 100 MHz): δ 169.8, 153.4, 148.1, 133.8, 131.5, 129.4, 120.6, 36.9, 31.8, 29.2, 29.1, 29.0, 23.4, 22.5, 13.2; FABMS m/z 279.3 $[M+H]^+$. Compound **3** (24%): White powder; ^{1}H NMR (CD_3OD, 400 MHz): δ 0.86 (t, J = 7.2 Hz, 3H), 1.18–1.26 (m, 12H), 2.10 (brs, 2H), 6.98 (d, J = 8.0 Hz, 2H), 7.5 (brs, 1H); ^{13}C NMR (CD_3OD, 100 MHz): δ 169.8, 158.3, 150.8, 136.1, 131.5, 118.4, 113.6, 36.9, 31.8, 29.2, 29.1, 29.0, 23.4, 22.5, 13.2; FABMS m/z 279.3 $[M+H]^+$. Compound **4** (11%): White powder; ^{1}H NMR (CD_3OD, 400 MHz): δ 0.82 (t, J = 7.2 Hz, 6H), 1.19–1.24 (m, 24H), 2.01–2.03 (m, 2H), 2.14–2.16 (m, 2H), 7.03 (d, J = 7.6 Hz, 1H), 7.25 (d, J = 7.6 Hz, 1H), 7.34 (t, J = 7.6 Hz, 1H); ^{13}C NMR ($CDCl_3$, 100 MHz): δ 170.7, 150.1, 138.2, 130.6, 129.7, 120.1, 118.0, 90.8, 37.1, 32.0, 29.9, 29.7, 29.5, 29.4, 23.5, 22.8, 14.3; FABMS m/z 375.5 $[M+H]^+$. Compound **5** (12%): White powder; ^{1}H NMR

(CD_3OD, 400 MHz): δ 0.83 (t, J = 7.2 Hz, 6H), 1.19–1.26 (m, 24H), 1.87 (m, 2H), 1.98 (m, 2H), 6.85 (m, 2H), 7.25 (t, J = 8.0 Hz, 1H); ^{13}C NMR ($CDCl_3$, 100 MHz): δ 156.6, 153.3, 137.0, 136.9, 115.2, 112.7, 112.0, 92.8, 37.1, 32.0, 29.9, 29.7, 29.5, 29.4, 23.5, 22.8, 14.3; FABMS m/z 375.5 $[M+H]^+$. Compound **6** (10%): White powder; ^1H NMR (CD_3OD, 400 MHz): δ 0.83 (t, J = 7.2 Hz, 3H), 1.25 (m, 12H), 1.67 (m, 1H), 2.0 (m, 1H), 5.46 (dd, J = 4.4, 8.0 Hz, 1H), 6.83 (d, J = 8.0 Hz, 1H), 6.94 (d, J = 7.2 Hz, 1H), 7.52 (t, J = 8.0 Hz, 1H); ^{13}C NMR ($CDCl_3$, 100 MHz): δ 170.8, 157.0, 152.5, 136.4, 115.4, 112.6, 81.5, 34.5, 31.8, 29.3, 29.2, 29.1, 24.5, 22.5, 13.2; FABMS m/z 263.3 $[M+H]^+$. Compound **7** (12%): White powder; ^1H NMR ($CDCl_3$, 400 MHz): δ 0.84 (t, J = 7.2 Hz, 3H), 1.25 (m, 12H), 1.68 (m, 1H), 2.01 (m, 1H), 5.49 (dd, J = 3.6, 8.0 Hz, 1H), 6.91 (m, 2H), 7.54 (dd, J = 6.0, 6.4 Hz, 1H), 7.80 (s, 1H); ^{13}C NMR (CD_3OD, 100 MHz): δ 172.4, 156.8, 150.7, 137.0, 115.5, 113.2, 111.4, 83.1, 34.8, 32.0, 29.9, 29.5, 29.5, 29.4, 25.0, 22.8, 14.3; FABMS m/z 263.3 $[M+H]^+$.

4.2.2. Preparation of 8

To a solution of 3-octyl-7-hydroxyphthalide (**7**; 5 mg, 0.018 mmol) in CH_3CN (1.5 ml), CH_3I (2.5 μl, ca. 0.04 mmol) and Ag_2O (8.5 mg, 0.04 mmol) were added, and the mixture was heated under reflux with stirring for 12 h. The solid material was removed by filtration, and the filtrate was evaporated to obtain a solid, which was purified by RP HPLC and eluted with 90% aqueous MeOH to give **8** (98%): white powder; ^1H NMR ($CDCl_3$, 400 MHz): δ 0.85 (t, J = 7.2 Hz, 3H), 1.23 (m, 12H), 1.68 (m, 1H), 1.97 (m, 1H), 3.97 (s, 3H), 5.35 (dd, J = 4.4, 8.0 Hz, 1H), 6.89 (d, J = 8.4 Hz, 2H), 6.93 (d, J = 7.2 Hz, 2H), 7.57 (t, J = 7.2, 8.4 Hz, 1H); ^{13}C NMR (CD_3OD, 100 MHz): δ 172.4, 156.8, 150.7, 137.0, 115.5, 113.2, 111.4, 83.1, 57.0, 34.8, 32.0, 29.9, 29.5, 29.5, 29.4, 25.0, 22.8, 14.3; FABMS m/z 277.3 $[M+H]^+$.

4.2.3. Preparation of 9 and 10

To a suspension of **3** (26 mg, 0.088 mmol), K_2CO_3 (12.3 mg, 0.088 mmol) and NaI (4.4 mg, 0.03 mmol) in DMF (3 ml) was added to benzyl chloride (20 μl, ca. 0.09 mmol), and the mixture was stirred for 30 min at 0 °C and for 4 h at room temperature. The mixture was acidified with aqueous 6 M HCl and extracted with EtOAc. The organic layer was successively washed with H_2O and brine, dried with $MgSO_4$, and evaporated to give a crude product, which was purified by RP HPLC eluting with 85% aqueous MeOH to give **9** and **10**. Compound **9** (20%): White powder; ^1H NMR (CD_3OD, 400 MHz): δ 0.87 (t, J = 7.2 Hz, 3H), 1.26 (m, 10H), 1.45 (m, 2H), 2.68 (dd, J = 7.2, 7.6 Hz, 2H), 5.12 (s, 2H), 5.24 (s, 2H), 7.35 (m, 12H), 7.58 (d, J = 8.0 Hz, 1H); ^{13}C NMR (CD_3OD, 100 MHz): δ 167.0, 154.1, 135.8, 129.7, 128.4, 128.4, 128.3, 120.9, 120.0, 67.2, 43.6, 31.8, 29.3, 29.1, 28,9, 23.1, 22.5, 13.2; FABMS m/z 459.4 $[M+H]^+$. Compound **10** (75%): White powder; ^1H NMR (CD_3OD, 400 MHz): δ 0.88 (t, J = 6.8 Hz, 3H), 1.25 (m, 10H), 1.52 (m, 2H), 2.72 (dd, J = 7.2, 7.6 Hz, 2H), 5.23 (s, 2H), 7.03 (d, J = 8.0 Hz, 1H), 7.35 (m, 7H); ^{13}C NMR (CD_3OD, 100 MHz): δ 166.3, 154.1, 135.8, 129.7, 128.4, 128.4, 128.3, 120.9, 120.0, 67.2, 43.6, 31.8, 29.3, 29.1, 28,9, 23.1, 22.5, 13.2; FABMS m/z 369.3 $[M+H]^+$.

4.2.4. Preparation of 11

To a solution of **10** (10 mg, 0.027 mmol) in CH_3CN (2 ml), CH_3I (3.4 μl, ca. 0.054 mmol) and Ag_2O (12.6 mg, 0.054 mmol) were added, and the mixture was heated under reflux with stirring for 12 h. After this time, the solid material was removed by filtration, and the filtrate was evaporated to obtain a solid, which was purified by RP HPLC eluting with 90% aqueous MeOH to give **11** (98%): white powder; ^1H NMR (CD_3OD, 400 MHz): δ 0.88 (t, J = 6.8 Hz, 3H), 1.25 (m, 10H), 1.52 (m, 2H), 2.72 (dd, J = 7.2, 7.6 Hz, 2H), 3.81 (s, 3H), 5.23 (s, 2H), 7.03 (d, J = 8.0 Hz, 1H), 7.35 (m, 7H); ^{13}C NMR (CD_3OD, 100 MHz): δ 166.3, 154.1, 135.8, 129.7, 128.43, 128.38, 128.25, 120.9, 120.0, 67.2, 56.3, 43.6, 31.8, 29.3, 29.1, 28,9, 23.1, 22.5, 13.2; FABMS m/z 263.3 $[M+H]^+$.

4.2.5. Preparation of 13 and 14

To a solution of phthalic anhydride (**12**) in THF at −20 °C, octylmagnesium bromide (2.5 equiv) in THF was added, and the reaction was stirred for 15 min and then warmed to room temperature for another 2 h. The reaction was quenched with 1 M HCl and concentrated in vacuo. The residue was diluted with EtOAc and successively washed with H_2O and brine. The organic layer was dried with $MgSO_4$ and evaporated to give a crude product, which was chomatographed on silica gel eluting with $CHCl_3$–MeOH to give **13** and **14**. Compound **13** (25%): Yellow oil; ^1H NMR ($CDCl_3$, 400 MHz): δ 0.84 (t, J = 7.2 Hz, 3H), 1.23 (m, 12H), 1.72 (m, 1H), 2.01 (m, 1H), 5.45 (dd, J = 4.1, 7.6 Hz, 1H), 7.41 (d, J = 7.6 Hz, 1H), 7.5 (t, J = 7.2 Hz, 1H), 7.65 (t, J = 7.6 Hz, 1H), 7.88 (d, J = 7.2 Hz, 1H); ^{13}C NMR ($CDCl_3$, 100 MHz): δ 170.7, 152.9, 134.1, 129.0, 125.8, 121.3, 90.6, 39.0, 32.0, 30.0, 29.8, 29.5, 29.3, 23.3, 22.8, 14.3; HRFABMS m/z 247.2738 $[M+H]^+$. Compound **14** (73%): Yellow oil; ^1H NMR ($CDCl_3$, 400 MHz): δ 0.82 (t, J = 7.2 Hz, 6H), 1.15 (m, 24H), 1.81 (m, 2H), 2.01 (m, 2H), 7.29 (d, J = 8.0 Hz, 1H), 7.47 (t, J = 8.0 Hz, 1H), 7.62 (t, J = 8.0 Hz, 1H), 7.83 (d, J = 8.0 Hz, 1H); ^{13}C NMR ($CDCl_3$, 100 MHz): δ 170.7, 152.9, 134.1, 129.0, 125.8, 121.3, 90.6, 39.0, 32.0, 30.0, 29.8, 29.5, 29.3, 23.3, 22.8, 14.3. FABMS m/z 359.3 $[M+H]^+$.

4.2.6. Preparation of 15 and 17

To a solution of **1** (16.4 mg, 0.1 mmol) or **16** (21 mg, 0.1 mmol) in aqueous CH_3CN (2 ml), 1-bromooctane (20 μl, ca. 0.12 mmol) and Ag_2O (46 mg, 0.2 mmol) were added, and the mixture was heated under reflux with stirring for 12 h. The solid material was removed by filtration, and the filtrate was evaporated to give a solid, which was purified by RP HPLC eluting with 90% aqueous MeOH to give **15** or **17**. Compound **15** (80%): white powder; ^1H NMR (CD_3OD, 400 MHz): δ 0.87 (t, J = 7.2 Hz, 3H), 1.28 (m, 10H), 1.70 (m, 2H), 4.23 (t, J = 6.8 Hz, 2H), 7.02 (d, J = 8.4 Hz, 1H), 7.06 (d, J = 7.2 Hz, 1H), 7.38 (dd, J = 7.6, 8.0 Hz, 1H); ^{13}C NMR (CD_3OD, 100 MHz): δ 170.9, 169.0, 158.9, 134.1, 132.4, 119.1, 118.8, 116.2, 65.7, 31.8, 29.1, 29.0, 28.3, 25.9, 22.5, 13.2; FABMS m/z 295.3 $[M+H]^+$. Compound **17** (80%): white powder; ^1H NMR (CD_3OD, 400 MHz): δ 0.87 (t, J = 6.8, 7.2 Hz, 3H), 1.29 (m, 10H), 1.75 (m, 2H), 4.29 (t, J = 6.8 Hz, 2H), 7.58 (t, J = 7.2, 8.4 Hz, 1H), 8.13 (d, J = 7.6 Hz, 1H), 8.16 (dd, J = 8.4 Hz, 1H); ^{13}C NMR (CD_3OD, 100 MHz): δ 171.1, 165.7, 146.8, 134.5, 130.1, 130.0, 128.2, 127.4, 66.0, 31.8, 29.2, 29.1, 28.4, 25.9, 22.5, 13.2; HRFABMS m/z 324.1314 $[M+H]^+$.

4.2.7. Preparation of 18 and 19

To a solution of **1** (16.4 mg, 0.1 mmol) in aqueous CH_3CN (2 ml), 1-bromooctane (20 μl, ca. 0.12 mmol) and Ag_2O (46 mg, 0.2 mmol) were added, and the mixture was heated under reflux with stirring for 12 h. After this time, the solid material was removed by filtration, and the filtrate was evaporated to give a solid. After methanol was added, the mixture was heated again at 35 °C for 30 min, evaporated to get the crude products, and purified by RP HPLC eluting with 90% aqueous MeOH to give **18** and **19**. Compound **18** (45%): white powder; ^1H NMR ($CDCl_3$, 400 MHz): δ 0.86 (t, J = 7.2 Hz, 3H), 1.26 (m, 8H), 1.40 (m, 2H), 1.75 (m, 2H), 3.89 (s, 3H), 3.99 (t, J = 6.4 Hz, 2H), 7.12 (d, J = 8.4 Hz, 1H), 7.39 (t, J = 8.0 Hz, 1H), 7.63 (d, J = 8.4 Hz, 1H); ^{13}C NMR (CD_3OD, 100 MHz): δ 170.9, 166.4, 158.9, 128.2, 126.8, 121.3, 119.1, 116.8, 69.1, 51.5, 31.8, 29.1, 29.0, 28.3, 25.9, 22.5, 13.2; FABMS m/z 309.5 $[M+H]^+$. Compound **19** (40%): white powder; ^1H NMR (CD_3OD, 400 MHz): δ 0.85 (t, J = 7.2 Hz, 3H), 1.23 (m, 8H), 1.42 (m, 2H), 1.80 (m, 2H), 3.89 (s, 3H), 4.06 (t, J = 6.4, 6.8 Hz, 2H), 7.11 (d, J = 8.0 Hz, 1H), 7.42 (t, J = 8.0 Hz, 1H), 7.49 (d, J = 7.6 Hz, 1H); ^{13}C NMR (CD_3OD,

100 MHz): δ 169.2, 167.2, 156.1, 130.3, 129.7, 125.6, 121.7, 116.5, 69.0, 51.7, 31.8, 29.5, 29.2, 29.1, 29.0, 25.8, 22.5, 13.2; FABMS *m*/*z* 309.5 $[M+H]^+$.

4.2.8. Preparation of 20

Decanoyl chloride (20 μl, ca. 0.1 mmol) in THF (2 ml) was cooled to 0 °C, and a solution of **1** (16.4 mg, 0.1 mmol) in THF (1.5 ml) was added dropwise; the mixture was stirred under 15 °C for 4 h. After this time, water was added and extracted with dichloromethane, then successively washed with H_2O and brine. The organic layer was dried with $MgSO_4$, and evaporated to give a crude product, which was chomatographed on silica gel eluting with $CHCl_3$-MeOH to give **20** (70%): white oil; ^1H NMR ($CDCl_3$, 400 MHz): δ 0.84 (t, *J* = 7.2 Hz, 3H), 1.23 (m, 12H), 1.72 (m, 2H), 2.24 (t, *J* = 6.4 Hz, 2H), 6.62 (d, *J* = 7.6 Hz, 1H), 6.64 (d, *J* = 8.0 Hz, 1H), 7.14 (t, *J* = 8.0 Hz, 1H); ^{13}C NMR ($CDCl_3$, 100 MHz): δ 172.3, 163.7, 163.5, 154, 143.1, 134.3, 130.1, 127.0, 126.7, 33.5, 31.9, 29.7, 29.4, 29.1, 25.1, 22.8, 14.1; HRFABMS *m*/*z* 319.1381 $[M+H]^+$.

4.3. Biological evaluations

4.3.1. Competitive binding assays

PPAR-γ binding was assessed according to the manufacturer's instructions (LanthaScreen, Invitrogen). In brief, 40 μl of the total reaction kit contained 0.5 nM PPAR-γ LBD (GST), 5 nM terbium-tagged anti-GST antibody, 5 nM Fluormone™ Pan-PPAR Green, and varying concentrations of rosiglitazone (10 nM–1000 μM). The negative control did not include the agonist. After 4-h incubation in the dark, TR-FRET measurements were performed using a TriStar LB941 spectrofluorometer (Berthold Technologies, Calmbacher, Germany) with the following settings: optical module, LanthaScreen; counting time, 0.1 s; and integration time, 20 μs. The ratiometric emission at 520/495 nm was plotted against various agonist concentrations. The data were analyzed using Prism software (GraphPad Software, Inc., San Diego, CA, USA).

4.3.2. Luciferase transactivation assays

Rat liver Ac2F cells were obtained from the American Type Culture Collection (ATCC, Rockville, MD, USA). The Ac2F cells were grown in Dulbecco's Modified Eagle Medium (DMEM, Nissui, Tokyo, Japan) containing 2 mM L-glutamine, 100 mg/ml streptomycin, 2.5 mg/L amphotericin B, and 10% heat-inactivated fetal bovine serum (FBS). Cells were maintained in a humidified atmosphere containing 5% CO_2 at 37 °C and were discarded after 3 months, at which time new cells were obtained from a frozen stock. Cells in the exponential phase were used for all experiments. The 3×AOX-TK-luciferase reporter plasmid containing three copies of the PPAR response element (PPRE) in the acyl CoA oxidase promoter was a kind gift from Dr. Chistopher K. Glass (University of California at San Diego, La Jolla, CA, USA). The pcDNA3 expression vector and full-length human PPAR-γ1 expression vector (pFlag-PPAR-γ1) were kind gifts from Dr. Chatterjee (University of Cambridge, Addenbrooke's Hospital at Cambridge, UK). The Lipofectamine™ 2000 transfection reagent was obtained from Invitrogen Co. (Carlsbad, CA, USA). Opti-MEM was obtained from Gibco (Grand Island, NY, USA).

For luciferase assays, 0.02 μg of plasmids was transfected into Ac2F cells in a 48-well plate (1×10^5 cells/well) with proper combinations of effector plasmids, 3×AOX-TK-luciferase reporter plasmid, pcDNA3, and pFlag-PPAR-γ1, by using Lipofectamine™ 2000 per the manufacturer's instructions. After transfection for 24 h, the conditioned media was removed and replaced with serum-free media and chemicals were added. After additional incubation for 6 h, cells were washed with PBS and assayed with the Steady-Glo Luciferase Assay System (Promega, Madison, WI, USA). Luciferase activity was measured using a GloMax®-Multi Microplate Multimode Reader (Promega Corporation, CA, USA).

ANOVA was used to determine significant differences between groups. Differences among the mean of individual groups were assessed by the Fisher's protected LSD post hoc test. Values of $p < 0.05$ were considered statistically significant.

4.4. Molecular modeling

Docking calculations were performed using AutoDock Vina 1.1.2 software.[27] The default settings and scoring function of Vina were applied. For ligand preparation, Chem3D Ultra 8.0 software was used to convert the 2D structures of the candidates into 3D structural data. Protein coordinates were downloaded from the Protein Data Bank, accession code 2PRG. Chain A was prepared for docking within the molecular modeling software package Chimera 1.5.3 by removing chain B, as well as all ligands and water molecules (except water molecules 308, 399, 444, and 467) and by calculating the protonation state of the protein. Addition of polar hydrogen and setting grid box parameters was performed by MGLTools 1.5.4. PyMol v1.5 was used for analyzing and visually investigating the ligand–protein interactions of the docking poses.

Acknowledgements

This study was supported by a Grant from the Marine Biotechnology Program funded by the Ministry of Land, Transport, and Maritime Affairs, and by a Grant from the National Research Foundation (No. 20090083538), Korea.

Supplementary data

Supplementary data associated with this article can be found, in the online version, at http://dx.doi.org/10.1016/j.bmc.2012.06.039.

References and notes

1. Evans, R. M.; Barish, G. D.; Wang, Y. X. *Nat. Med.* **2004**, *10*, 355.
2. Berger, J.; Moller, D. E. *Annu. Rev. Med.* **2002**, *53*, 409.
3. Mangelsdorf, D. J.; Thummel, C.; Beato, M.; Herrlich, P.; Schötz, G.; Umesono, K.; Blumberg, B.; Kastner, P.; Mark, M.; Chambon, P.; Evans, R. M. *Cell* **1995**, *83*, 835.
4. Nuclear receptors nomenclature committee. *Cell* **1999**, *97*, 161.
5. Spiegelman, B. M. *Diabetes* **1998**, *47*, 507.
6. Henke, B. R.; Blanchard, S. G.; Brackeen, M. F.; Brown, K. K.; Cobb, J. E.; Collins, J. L., ; Harrington, W. W., Jr.; Hashim, M. A.; Hull-Ryde, E. A.; Kaldor, I.; Kliewer, S. A.; Lake, D. H.; Leesnitzer, L. M.; Lehmann, J. M.; Lenhard, J. M.; Orband-Miller, L. A.; Miller, J. F.; Mook, R. A., Jr.; Noble, S. A.; Oliver, W., Jr.; Parks, D. J.; Plunket, K. D.; Szewczyk, J. R.; Willson, T. M. *J. Med. Chem.* **1998**, *41*, 5020.
7. Collins, J. L.; Blanchard, S. G.; Boswell, G. E.; Charifson, P. S.; Cobb, J. E.; Henke, B. R.; Hull-Ryde, E. A.; Kazmierski, W. M.; Lake, D. H.; Leesnitzer, L. M.; Lehmann, J.; Lenhard, J. M.; Orband-Miller, L. A.; Gray-Nunez, Y.; Parks, D. J.; Plunkett, K. D.; Tong, W. Q. *J. Med. Chem.* **1998**, *41*, 5037.
8. Cobb, J. E.; Blanchard, S. G.; Boswell, E. G.; Brown, K. K.; Charifson, P. S.; Cooper, J. P.; Collins, J. L.; Dezube, M.; Henke, B. R.; Hull-Ryde, E. A.; Lake, D. H.; Lenhard, J. M.; Oliver, W., Jr.; Oplinger, J.; Pentti, M.; Parks, D. J.; Plunket, K. D.; Tong, W. Q. *J. Med. Chem.* **1998**, *41*, 5055.
9. Willson, T. M.; Wahli, W. *Curr. Opin. Chem. Biol.* **1997**, *1*, 235.
10. Nolte, R. T.; Wisely, G. B.; Westin, S.; Cobb, J. E.; Lambert, M. H.; Kurokawa, R.; Rosenfeld, M. G.; Willson, T. M.; Glass, C. K.; Milburn, M. V. *Nature* **1998**, *395*, 137.
11. Edwards, I. J.; O'Flaherty, J. T. *PPAR Res.* **2008**, *2008*, 1.
12. Willson, T. M.; Brown, P. J.; Sternbach, D. D.; Henke, B. R. *J. Med. Chem.* **2000**, *43*, 527.
13. Kuhn, B.; Hilpert, H.; Benz, J.; Binggeli, A.; Grether, U.; Humm, R.; Marki, H. P.; Meyer, M.; Moh, P. *Bioorg. Med. Chem. Lett.* **2006**, *16*, 4016.
14. Xu, H. E.; Lambert, M. H.; Montana, V. G.; Plunket, K. D.; Moore, L. B.; Collins, J. L.; Oplinger, J. A.; Kliewer, S. A.; Gampe, R. T., Jr.; McKee, D. D.; Moore, J. T.; Willson, T. M. *Proc. Natl. Acad. Sci. U.S.A.* **2001**, *98*, 13919.
15. Liu, J.; Li, F. M.; Kim, E. L.; Li, J. L.; Hong, J. K.; Bae, K. S.; Chung, H. Y.; Kim; H, S.; Jung, J. H. *J. Nat. Prod.* **2011**, *74*, 1826.
16. Wang, Y.; De, S. A.; Schuler, G.; D'orazio, D.; Raderatorff, D.; Wolfram, S.; Weber, P.; Teixeira, S. EP 1 622 605, 2004; Maria, Y. R.; Guillermo, D.; Ruben, A. T. *Tetrahedron* **1998**, *54*, 3355.

17. Tomoya, O.; Kenji, M. *Biosci. Biotechnol. Biochem.* **2003**, *67*, 2240–2244.
18. Tomoya, O.; Kenji, M. *Biosci. Biotechnol. Biochem.* **2001**, *65*, 172.
19. Noller, C. R. *Chemistry of Organic Compounds*, 3rd ed.; W.B. Saunders: Philadelphia, 1965. p 602.
20. Cronet, P.; Petersen, J. F.; Folmer, R.; Blomberg, N.; Sjöblom, K.; Karlsson, U.; Lindstedt, E. L.; Bamberg, K. *Structure* **2001**, *9*, 699.
21. Markt, P.; Schuster, D.; Kirchmair, J.; Laggner, C.; Langer, T. *J. Comput. Aided Mol. Des.* **2007**, *21*, 575.
22. Kroemer, R. T.; Vulpetti, A.; McDonald, J. J.; Roher, D. C.; Trosset, J. Y.; Giordanetto, F.; Cotesta, S.; McMartin, C.; Kihlen, M.; Stouten, P. F. W. *J. Chem. Inf. Comput. Sci.* **2004**, *44*, 871.
23. Porcelli, L.; Gilardi, F.; Laghezza, A.; Piemontese, L.; Mitro, N.; Azzariti, A.; Altieri, F.; Cervoni, L.; Fracchiolla, G.; Giudici, M.; Guerrini, U.; Lavecchia, A.; Montanari, R.; Di; Giovanni, C.; Paradiso, A.; Pochetti, G.; Simone, G. M.; Tortorella, P.; Crestani, M.; Loiodice, F. *J. Med. Chem* **2012**, *55*. 37.
24. Warren, G. L.; Andrews, C. W.; Capelli, A.-M.; Clarke, B.; LaLonde, J.; Lambert, M. H.; Lindvall, M.; Nevins, N.; Semus, S. F.; Senger, S.; Tedesco, G.; Wall, I. D.; Woolven, J. M.; Peishoff, C. E.; Head, M. S. *J. Med. Chem.* **2006**, *49*, 5912.
25. Takada, I.; Yu, R. T.; Xu, H. E.; Lambert, M. H.; Montana, V. G.; Kliewer, S. A.; Evans, R. M.; Umesono, K. *Mol. Endocrinol.* **2000**, *14*, 733.
26. Yanagisawa, H.; Takamura, M.; Yamada, E.; Fujita, S.; Fujiwara, T.; Yachi, M.; Isobe, A.; Hagisawa, Y. *Bioorg. Med. Chem. Lett.* **2000**, *10*, 373.
27. Trott, O.; Olson, A. J. *J. Comput. Chem.* **2010**, *31*, 455.